Road Materials and Pavement Design

ISSN: (Print) (Online) Journal homepage: https://www.tandfonline.com/loi/trmp20

Optimisation and field assessment of poroelastic wearing course bond quality

P. Jaskula, D. Rys, C. Szydłowski, M. Stienss, L. Mejlun, M. Jaczewski & G. Ronowski

To cite this article: P. Jaskula, D. Rys, C. Szydłowski, M. Stienss, L. Mejlun, M. Jaczewski & G. Ronowski (2021) Optimisation and field assessment of poroelastic wearing course bond quality, Road Materials and Pavement Design, 22:sup1, S604-S623, DOI: 10.1080/14680629.2021.1902844

To link to this article: https://doi.org/10.1080/14680629.2021.1902844

Published online: 26 Mar 2021.

ROAD MATERIALS AND PAVEMENT DESIGN
2021, VOL. 22, NO. S1, S604–S623
https://doi.org/10.1080/14680629.2021.1902844

Taylor & Francis
Taylor & Francis Group

Optimisation and field assessment of poroelastic wearing course bond quality

P. Jaskula [a], D. Rys [a], C. Szydłowski [a], M. Stienss [a], L. Mejlun [a], M. Jaczewski [a] and G. Ronowski [b]

[a]Faculty of Civil and Environmental Engineering, Gdansk University of Technology, Gdansk, Poland; [b]Mechanical Faculty, Gdansk University of Technology, Gdansk, Poland

ABSTRACT

Compared to typical asphalt mixtures, poroelastic mixtures are characterised by high porosity and high flexibility, which are desirable for traffic noise reduction. However, the same properties increase the risk of debonding from the lower layer, which is a significant source of premature damage. The study investigates which of the factors – tack coat agent, type and texture of the lower layer – have the greatest impact on interlayer bonding quality. From 27 variants of interface bond techniques investigated in laboratory, 8 were selected and constructed on two full-scale test sections. Monotonic direct shear loading and cyclic direct shear loading tests with normal force were used for this purpose. The tests indicated that softer bitumen used for the tack coat and the milled texture of the lower layer improves bond quality. However the appropriate laying compaction has the major influence. Poroelastic mixtures are much more sensitive to technological imperfections than standard asphalt mixtures.

ARTICLE HISTORY
Received 31 July 2020
Accepted 9 March 2021

KEYWORDS
Poroelastic layer; interlayer bonding; direct shear test; low-noise pavement; crumb rubber; highly polymer-modified bitumen

Introduction

Safe and Eco-Friendly Poroelastic Road Surface (SEPOR) is a low-noise wearing course for road pavements that incorporates specially designed aggregate skeleton made of crumb rubber and mineral aggregate (Jaskula et al., 2020). Highly polymer-modified (HiMA) bitumen is used as binder instead of polyurethane resin used in previous research (Goubert & Sandberg, 2009; Kalman et al., 2011; Lu et al., 2019; Meiarashi, 2004; Sandberg, 2015; Wang et al., 2017).

Poroelastic pavements are developed to reduce traffic noise at its source. In modern vehicles, tyre/road noise interaction is the dominant noise source at medium and high-speed driving (that is over 30–40 km/h). During the interaction between tyre and pavement, two groups of noise-generating mechanisms are active – aerodynamic and impact-related. A poroelastic road pavement reduces aerodynamic-related noise mechanisms (e.g. air-pumping) due to its porosity and mitigates impact-related mechanisms (such as vibrations of tread elements hitting road surface) due to its flexibility.

Poroelastic mixtures for road pavements contain about 20% of crumb rubber and are characterised by the open (porous) structure of the constructed layer. These mixtures are used for wearing courses exclusively. PERS (PoroElastic Road Surface) technology originates from Swedish research conducted in the 1970s. From 1994 research efforts on poroelastic pavements were also conducted in Japan, where a few generations of PERS were developed between 1994 and 2009 (Sandberg et al., 2010). First trials resulted in the reduction of pavement noise by 5 dB, while further research resulted in a

CONTACT D. Rys dawid.rys@pg.edu.pl

decrease by as much as 12 dB in comparison to reference SMA (stone matrix asphalt) wearing course (Świeczko-Żurek et al., 2018).

Noise is not the only environmental concern related to road traffic. The issue of CO_2 emission is of even greater importance nowadays. Emission is roughly proportional to the amount of energy needed to power vehicles. One of the most important resistance forces acting on all the moving vehicles is the rolling resistance (Ejsmont et al., 2015). Rolling resistance depends on tyre construction, road pavement characteristics and operating parameters. The goal of the SEPOR project is to provide poroelastic pavement that would not increase, but possibly reduce the rolling resistance. This is not an easy task, as energy losses in flexible pavement are more difficult to control than in rigid pavement. Unfortunately, at the present state of development, the rolling resistance of car tyres on SEPOR at 20°C is up to 15% higher than on reference pavements like SMA8. At low temperatures, however, the difference is much lower – for example at 10°C rolling resistance on SEPOR is only 10% higher than on SMA8. While it proved impossible to perform road tests at lower temperatures so far, laboratory drum measurements indicate that for temperatures about 0°C, rolling resistance on SEPOR is similar to resistance on SMA8.

The greatest drawback of the poroelastic layer noted during previous studies was its very low durability – in some cases the pavement lasted only a few weeks before critical deterioration occurred. Ravelling and debonding from the lower layer were identified as the primary causes of insufficient durability (Bendtsen, 2015; Sandberg, 2015). Despite excellent properties in terms of noise reduction (Ejsmont et al., 2016, 2019; 2014a, 2014b), insufficient durability still renders PERS technology useless in practical conditions.

Knowledge about the mechanisms of deboning of poroelastic layers or the properties of layer interfaces, which would ensure higher durability, is still very limited. Literature review shows (Srirangam et al., 2016) that a decrease in difference in stiffness between two layers has a detrimental effect on the durability of their bonding. However, previous research has shown that in the case of a poroelastic layer used as a wearing course stiffness is at least 5–15 times lower than in the case of a standard asphalt wearing course placed on traditional asphalt mixture (Ejsmont et al., 2018; Jaskula et al., 2019; Sandberg et al., 2010; Świeczko-Żurek et al., 2015). This property could have a detrimental effect on the quality of interlayer bond and premature failure of the PERS trial sections.

The aim of the presented study was to improve bond durability between the poroelastic layer SEPOR and the lower asphalt layer. For this purpose, direct shear test with monotonic load and its further modifications with cyclic load were used at the laboratory stage for 27 variants of interface bond techniques. Conclusions formulated after this stage were later practically verified on two field test sections with eight selected interfaces subjected to real traffic, in order to identify the properties that correspond to the observed distresses to the greatest degree.

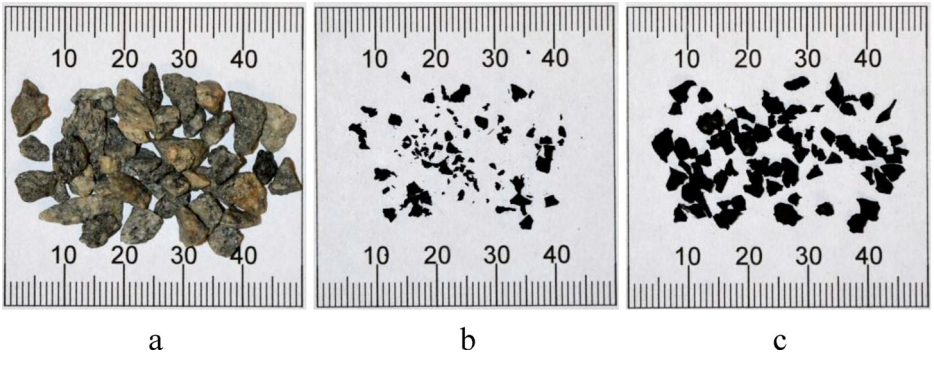

Figure 1. Mineral and crumb rubber materials used in the tests: (a) gneiss coarse aggregate 2/5; (b) crumb rubber 0.5/2; (c) crumb rubber 1/4.

Table 1. Properties of highly modified bitumen (HiMA).

Property		45/80-80
Penetration at 25°C, 0.1 mm, acc. to PN-EN 1426	Original	53
	RTFO	40
R&B Temperature, [°C], acc. to PN-EN 1427	Original	78.7
	RTFO	87.8
Performance Grade,acc. to AASHTO M 320		PG 82–22
Resistance to heavy traffic load, acc. to AASHTO M 332		E

Materials

Mineral-crumb rubber mixture

The mineral part of the poroelastic mixture that was investigated contained coarse crushed gneiss aggregate, fine gneiss aggregate and limestone filler. The rubber part of the mixture was composed of crumb rubber obtained from tyre recycling. The recycling process used shredding technique at ambient temperature. Two different fractions of crumb rubber were used in this study: 0.5/2 and 1/4. Coarse crushed gneiss aggregate of the 2/5 mm fraction and crumb rubber of different sizes are shown in Figure 1.

Bitumen

Instead of polyurethane epoxy resins used as binders in previous research programmes, highly modified bitumen (HiMA) 45/80–80, containing approximately 7% of SBS, was used. The properties of bitumen produced in one of Polish refineries are shown in Table 1.

Poroelastic mineral-crumb rubber asphalt mixture

During the optimisation of the SEPOR mixture, many different variants were tested in terms of their performance properties, water permeability and noise reduction capabilities. The mineral skeleton of those mixtures was based on traditional asphalt mixtures: stone matrix asphalt, porous asphalt and gap-graded asphalt mixture, whose compositions were based on Polish and Swedish technical regulations concerning the mineral gradation of asphalt mixtures. The mixture used for the poroelastic layer was labelled as PSMA 5 (poroelastic SMA) and consisted of mineral aggregate, crumb rubber aggregate, limestone filler and highly polymer-modified asphalt binder 45/80-80. For the process of optimisation of interlayer bond quality, one poroelastic mixture, designated as SEPOR-PSMA5 W4, was selected. A more detailed description of properties, and optimisation process of all the tested poroelastic mixtures, was presented in the previous study (Jaskula et al., 2019). The proportions of components are given in Table 2. Figure 2 presents the grading curve of PSMA 5 mixture and grading envelope for typical SMA 5 mixture. Poroelastic mixtures PSMA 5 with different binder contents were tested. During laboratory stage, poroelastic mixture with 11% binder content was investigated. Field trial sections were constructed with different binder contents: 9% on section 1, 11% and 13% on Section 2. After the preliminary trials, it was established that two parameters would be considered in the initial phase of the selection process: (1) air void content, (2) internal (in-layer) shear strength obtained from the Leutner apparatus. The results of those tests for poroelastic mixture PSMA5 W4 with various binder contents are presented in Figure 3. It was assumed that the internal shear strength is mainly responsible for the durability of the mixture in the field. Only mixtures that achieved the target levels of these two parameters (minimum air void content 15%, minimum internal shear strength $\tau = 0.7$ MPa at $+20$°C) were selected.

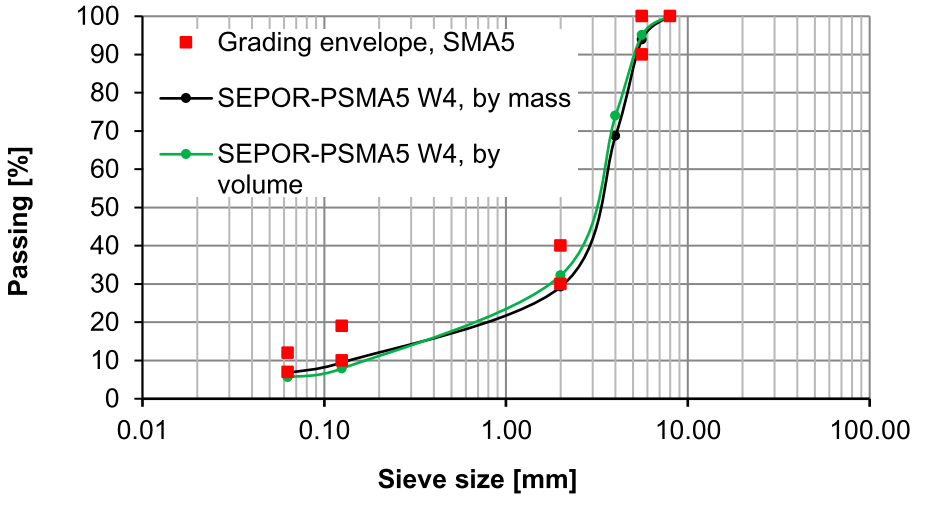

Figure 2. SEPOR-PSMA5 W4 grading curve.

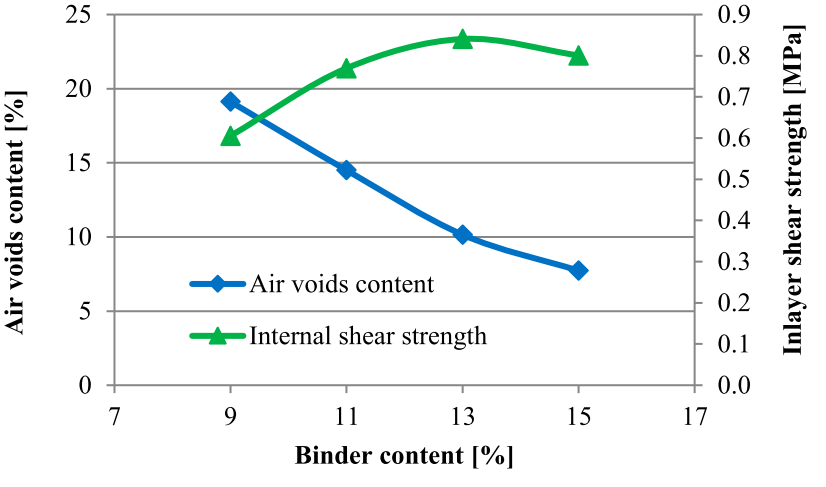

Figure 3. Results of air void content and internal (in-layer) shear strength of the mixture SEPOR-PSMA5 W4 with various binder contents.

It should be emphasised that the poroelastic mixture PSMA 5 exhibits much lower stiffness (around 200 MPa) in comparison to 1400 MPa obtained for the reference SMA 11 (IT-CY test at 25°C, according to EN 12697-26). Analogously, internal shear strength (at 20°C, according to EN 12697-48) results were as follows: 0.77 MPa for PSMA 5 and 1.81 MPa for the reference SMA 11.

Methodology

Description of the experiment

At the initial planning stages of the experiment, only a general outline of the problem was known – that is the potential delamination of the poroelastic layer from the underlying pavement courses. The industrial partner of the SEPOR project considered it necessary to test other bonding techniques as well, including laying of the SEPOR course over a milled bituminous layer with coarse grooves. The bonding quality was assessed using the direct shear test under monotonic load as well as the cyclic

Table 2. SEPOR-PSMA5 W4 poroelastic mixture composition.

Mix ingredient	Rubber-mineral aggregate mix [%]	Asphalt-rubber-mineral aggregate mix (by mass) [%]		
Coarse aggregate 2/5	72	65.2	63.8	62.4
Fine aggregate 0/2	6	5.4	5.3	5.2
Limestone filler	7	6.3	6.2	6.1
Crumb rubber $\frac{1}{4}$	10	9.1	8.9	8.7
Crumb rubber 0.5/2	5	4.5	4.4	4.3
Cellulose fibres	-	0.4	0.4	0.4
45/80-80 Binder	-	9.0	11.0	13.0

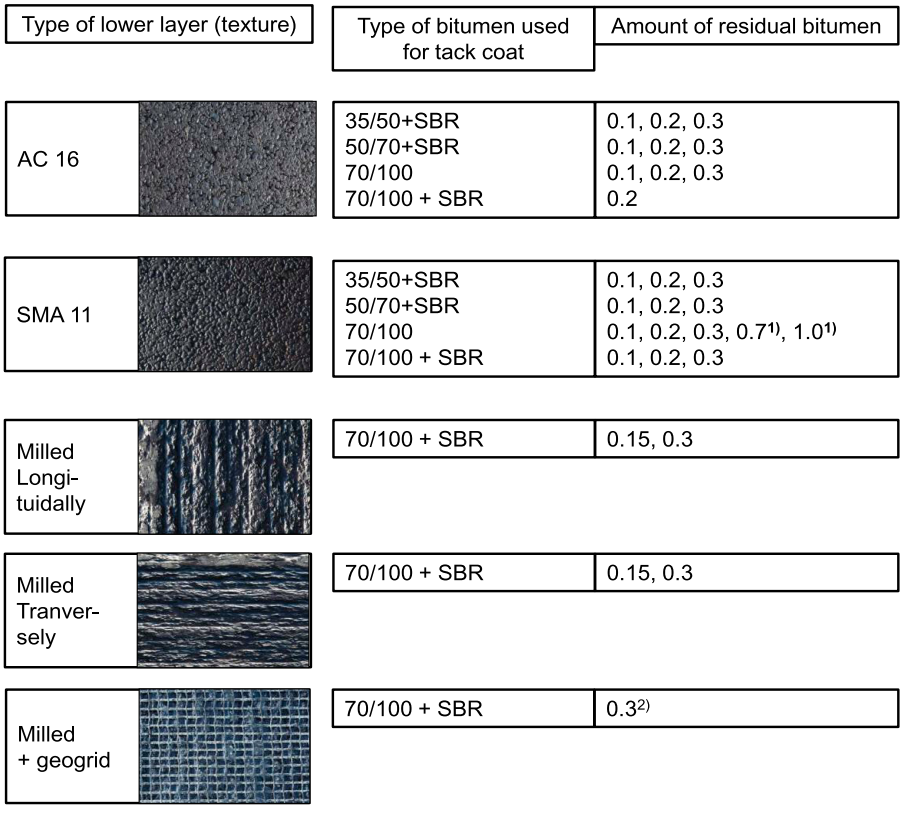

Figure 4. Combinations of bonding techniques used in the study.

direct shear test in the Advanced Shear Tester (AST) device, developed by Zofka et al. (2014 august, 2015). The performed tests and the obtained parameters are described in further parts of the paper.

At the first stage of laboratory testing, over a dozen different interlayer combinations were tested. These combinations are shown in Figure 4. The aim of the preliminary tests was to determine not only the factors that affect the strength and durability of the interlayer bond to the greatest degree, but also those whose impact is negligible. Based on the laboratory tests, interface variants for further testing on full-scale test sections were designated. The constructed test sections were subjected to observation and assessment in terms of distress caused by complete or partial loss of interlayer bonding.

The results were analysed in the following order:

(1) Determination of the effect of residual bitumen amount after the application of tack coat;

(2) Identification of the effect of bitumen type used;
(3) Analysis of the impact of the texture and type of the lower layer.

As shown in Figure 4, the following types of the lower Hot Mix Asphalt (HMA) layer were analysed:

- AC 16 W with 35/50 road bitumen, with a standard surface texture typically obtained after compaction with drum roller compactor,
- SMA 11 with PMB 45/80-55 modified bitumen, with various surface texture combinations: standard, grooved longitudinally or transversely (due to milling) as well as milled and covered with carbon/glass fibre reinforcement.

The tack coat was applied by spraying the interface with the following types of bituminous materials:

- Bituminous emulsion C60B3 70/100
- Bituminous emulsion C60BP3 70/100 with SBR polymer
- Bituminous emulsion C60BP3 50/70 with SBR polymer
- Bituminous emulsion C60BP3 35/50 with SBR polymer
- Hot bitumen 70/100

Application rates of the bituminous emulsions were set in order to obtain the following amounts of residual bitumen: 0.1, 0.2 or 0.3 kg/m^2 for specimens without grooves and 0.15 or 0.3 kg/m^2 for specimens with grooves. All the emulsions used were dedicated for interlayer bonds. For the application of hot bitumen, 0.7 and 1.0 kg/m^2 for specimens were taken into account, to verify the impact of a higher amount of binder on bond quality. Such a high amount of binder cannot be applied with the use of asphalt emulsion. Moreover, the influence of placement of pre-bituminised carbon/glass fibre grid at the interface was also evaluated. The function of the grid was to reinforce the bottom of the poroelastic layer. In total, specimens, representing 27 combinations of layer interfaces, were tested in the preliminary laboratory tests. For each combination, two specimens were tested. Based on the results, six combinations were selected for the construction on full-scale test sections.

Two test sections were constructed. Six combinations of interlayer bonds were tested in the field. Specimens were cored and subjected to laboratory tests analogous to those performed during the preliminary testing. As reference, typical interlayer bond between SMA8 wearing course and AC 16 binder course was additionally constructed in the field at the same time as the poroelastic pavements. Both test sections were put into operation and subjected to typical road traffic, with AADT equal to 150 and 1740 vehicles/day/lane, respectively. Through systematic monitoring of pavement condition on test sections, information, regarding processes leading to distress of the poroelastic layer, was collected.

The performed experiment resulted in the identification of interlayer bonding techniques that provide high durability of bond between the poroelastic layer and the underlying layer. Parameters that may be determined based on shear tests were also verified in terms of their correlations with distress observed on the test sections in field.

Laboratory tests

Sample preparation

During the preliminary laboratory testing, double-layer circular specimens were used with a diameter of 100 or 150 mm and a total thickness of 80 mm (40 mm per layer). While the lower layers differed in their textures, the upper poroelastic layers were always the same. The specimens were prepared according to the following procedure:

- Asphalt mixtures for the lower layer were produced on an industrial scale in an asphalt plant and compacted in a laboratory roller compactor;

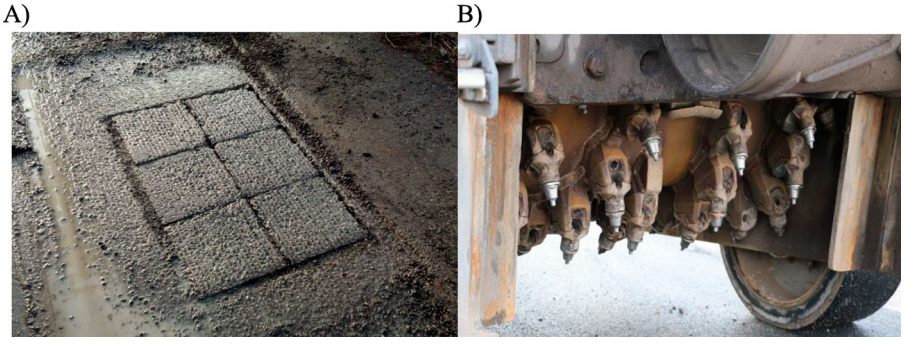

Figure 5. (A) A view of the 30 × 30 × 8 cm plates located in a hollow in an existing pavement just after milling; (B) a view of the milling drum of the cold milling machine used for specimen preparation.

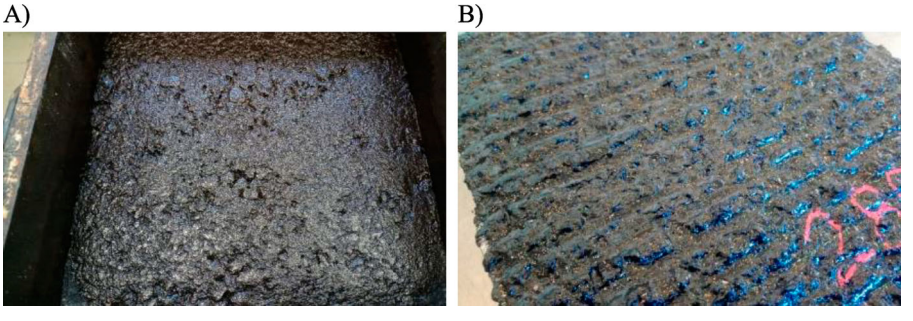

Figure 6. The lower HMA layer with visible tack coat after emulsion setting: (A) the unmilled lower layer; (B) milled surface of the lower layer.

Figure 7. Coring of cylindrical specimens with a laboratory drill and an exemplary plate with cored 100 and 150 mm specimens.

- Chosen specimens were placed in a specially prepared shallow pit (approx. 3 cm deep) located in the pavement and then underwent the milling process by the normal cold milling machine to obtain the same texture of the upper surface as it would be in real construction conditions (Figure 5);
- Surfaces were sprayed with bituminous emulsion or brushed with hot bitumen at the set amount in order to form the tack coat (Figure 6);
- Hot poroelastic mix was laid on the prepared surfaces and compacted with the laboratory roller compactor. Thickness of the poroelastic layer after compaction equalled 4 cm;
- Cylindrical specimens of 100 and 150 mm in diameter were cored from the compacted plates using a laboratory core driller (Figure 7).

Figure 8. General view of the shearing device for interlayer bonding testing (Leutner device).

Monotonic direct shear loading test

Interlayer bonding and in-layer shearing strength under monotonic loading was assessed using the direct shear test method, proposed by Leutner in 1979 (FGSV, 1999), see Figure 8 and propagated by others (Mohammad et al., 2009; Raab & Partl, 1998; Recasens et al., 2006; Sholar, 2004). While the original procedure assumes that the distance between the shearing clamps is equal to 0 mm, in the presented test the distance was set to 2 mm, which enables significant elimination of aggregate shearing. Directly before the test the specimens were conditioned for 12 h at +20°C. Shearing in the assumed failure plane progresses at the set displacement rate of 50 mm/min, up to the point of maximum shearing force and further, until complete shearing failure of the interface occurs. 100 mm diameter samples were used for the monotonic direct shear test.

The shearing strength of the interface $\tau_{\max}$ is calculated from the maximum registered shearing force divided by the area of the cross-section.

Additional bonding assessment was based on shearing failure energy W_m, Equation (1) (Hakimzadeh et al., 2012; Jia & Huang, 2015),

$$W_m = \int_0^{\delta f} \tau(\delta) d\delta \tag{1}$$

where W_m – work (energy) needed to cause failure of the interlayer bond in monotonic shearing test [kJ/m^2], $\tau(\delta)$ – shearing stress [kPa] as a function of shearing displacement δ [m], δ_f – failure point. The moment of failure was assumed as the moment when the force reaches 10% of the registered maximum value, which corresponds to the moment of complete shearing failure.

Cyclic direct shear loading test with normal force

Cyclic direct shear testing was performed using the Advanced Shear Tester (abbreviated to AST). The AST device enables application of shear load with normal confinement, as presented in Figure 9. The device is described in greater detail in Zofka et al. (2014 august, 2015). Similarly as in other studies (Crispino et al., 1997; Donovan et al., 2000; D'Andrea et al., 2013; Górszczyk & Malicki, 2012; Kruntcheva et al., 2004; Mohammad et al., 2009; Ragni et al., 2020; Romanoschi & Metcalf, 2001), the scheme of direct shearing with normal stress was used in the AST device.

The following loading conditions were used in the cyclic shear test of 150 mm diameter samples, based on the previous research (Jaskula, 2018)

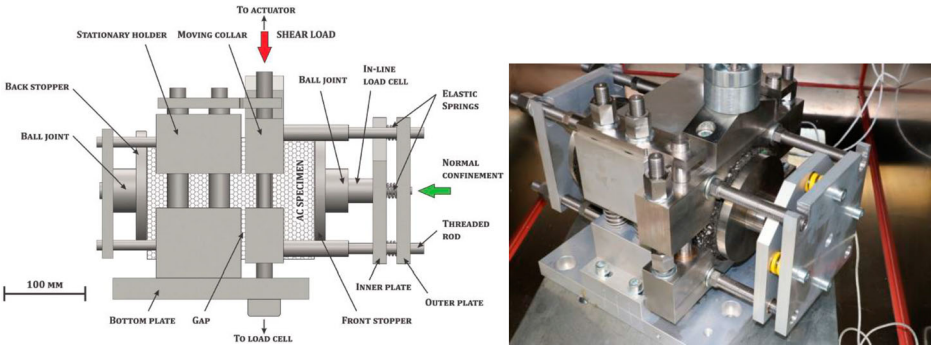

Figure 9. AST device used in interlayer bonding testing on circular specimens with 150 mm diameter under the loading scheme with additional normal load (force perpendicular to the shearing plane). Scheme of the device after (Zofka et al., 2015).

- Sinusoidal type of loading with rest time;
- Loading time equals 0.05 s, unloading 0.05 s and rest time equals 0.1 s, resulting in a full cycle of 0.2 s;
- Minimum shearing force during rest $F_{\min} = 0.9$ kN, which corresponds to shearing stress of $\tau_{\min} = 50$ kPa;
- Maximum shearing force $F_{\max} = 2.7$ kN, which corresponds to maximum shearing stress of $\tau_{\max} = 150$ kPa;
- Normal stress equals to 45 kPa, which constitutes 30% of shearing stress;
- Test temperature of 20°C.

Changes of force and displacement were registered in every cycle. Force was converted to shearing stress τ. The values of strain presented in Figure 10 were standardised and the strain value 0 was assigned to the beginning of the cycle. Based on the changes of shear stress vs. strain in a given cycle, hysteresis loops were plotted. Figure 10 shows examples of hysteresis loops for the 10th, 20th, 100th, 1000th and 10,000th cycles. Their shapes change in consecutive cycles. The area within the hysteresis loop reflects the work performed in the particular cycle, which, according to the law of conservation of energy, is dissipated in the material.

The slope of the line passing through the point of minimum stress/strain and the point of maximum stress/strain in the cycle corresponds to the shear resilient modulus in that cycle.

During the shear test the following values were calculated for every load cycle:

- Total permanent strain accumulated from the start of the test ϵ_p,
- Shear modulus K_p and shear resilient modulus K_r,
- Total dissipated energy from the start of the test W_c.

Shear modulus K_p and shear resilient modulus K_r were calculated according to Equations (2) and (3), respectively. The shear modulus $K_{p,i}$ in the ith cycle is calculated with regard to the total accumulated strain. In contrast, the shear resilient modulus $K_{r,i}$ is determined on the basis of resilient strain in a given ith cycle. The resilient strain is obtained from the difference between the maximum and minimum strains registered during the cycle.

$$K_{p,i} = \frac{4F_{\max,i}}{\pi D^2 \varepsilon_{p,i}} \tag{2}$$

$$K_{r,i} = \frac{4(F_{\max,i} - F_{\min,i})}{\pi D^2 \varepsilon_{r,i}} \tag{3}$$

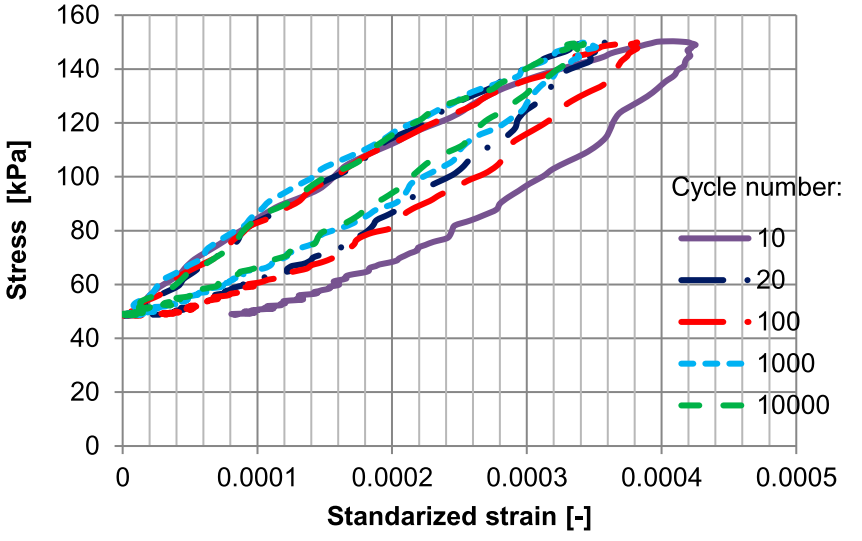

Figure 10. Examples of hysteresis loops – relative changes of shear stress and strain within the 2 s cycles of cyclic shear tests in the AST device.

where $K_{p,i}$ – shear modulus in the i-th cycle, $K_{r,i}$ – shear resilient modulus in the i-th cycle, $F_{\max,i}$, $F_{\min,i}$ – maximum and minimum force registered in the i-th cycle, respectively, $\epsilon_{p,i}$ – total permanent strain accumulated from the start of the test to the i-th cycle, $\epsilon_{r,i}$ – elastic strain in the i-th cycle, D – diameter of the tested specimen, equal to 150 mm.

The number of cycles N corresponding to the assumed decrease in shear modulus was used for the evaluation of interlayer bond under cyclic shearing. The moment of shearing failure was assumed as the decrease in shear modulus to the level of 25% of its initial value K_{ini}, that is the value registered in the 50th test cycle.

Dissipated energy in a given test cycle was calculated based on particular hysteresis loops, whose example shapes are shown in Figure 9. Dissipated energy in the i-th cycle W_i is defined by Equation (4). The dissipated energy may be interpreted graphically as the area within the hysteresis loop. In this analysis the energy was calculated as this area using raw test data.

$$W_i = \int_{\epsilon_{\min}}^{\epsilon_{\max}} \tau_L \mathrm{d}\varepsilon - \int_{\epsilon_{\max}}^{\epsilon_{\min}} \tau_U \mathrm{d}\varepsilon \tag{4}$$

where W_i – dissipated energy in the i-th test cycle [kJ/m^3], τ_L – shear stress as a function of standardised strain ϵ [kPa] during loading, τ_U – shear stress as a function of standardised strain ϵ [kPa] during unloading, $\epsilon_{\min}$ – minimum standardised strain, $\epsilon_{\max}$ – maximum standardised strain, at a given cycle i.

Total dissipated energy from the start of the test is defined by Equation (5).

$$W_c = \sum_{i=1}^{N} W_i \tag{5}$$

where W_c – total dissipated energy from the start of the test [kJ/m^3], N – number of cycles.

Results and discussion

Preliminary laboratory tests

At the stage of preliminary laboratory tests both interlayer bond shear strength in Leutner device and shear fatigue life in AST device were evaluated. Tests were performed for layer interface combinations

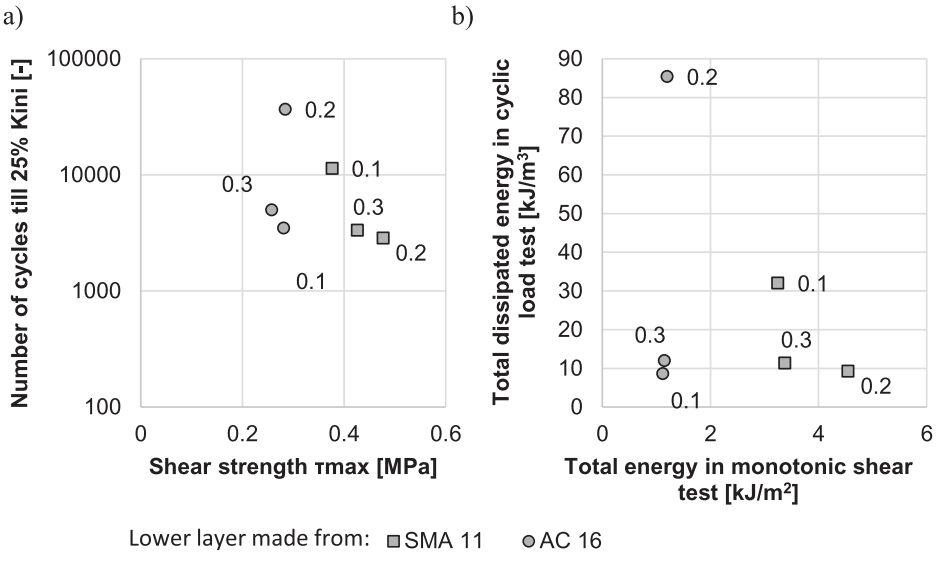

Figure 11. Chosen results of monotonic and cyclic shearing tests of interfaces between poroelastic layer and the lower layers of AC 16 or SMA 11.

shown in Figure 4. Results were grouped and analysed according to various criteria. The first criterion for comparisons was the amount of tack coat bitumen, with the same type of tack coat and the same type of underlying surface.

Results of preliminary laboratory tests are presented in Figures 11 and 12. The idea was to compare results of direct shear tests performed with monotonic and cyclic loads. Shear strength was compared to the number of cycles till failure (25% of K_{ini}). Total dissipated energy was also compared to total energy in shear test. Figure 11(a) shows example results of strength obtained in the monotonic shear test and bond shear fatigue life defined as $N_{25\%}$. Analogously, Figure 11(b) shows example results of total energy spent during monotonic shearing vs. total dissipated energy in the cyclic shear test. Results located closer to the upper right corner of the plot area in Figure 12(a,b) are more advantageous, as they imply greater strength and greater shear fatigue life of the interlayer bond. The results presented in Figure 11 were obtained for emulsion C60B3 70/100 and residual bitumen amounts after emulsion setting of 0.1, 0.2 and 0.3 kg/m^2, labelled accordingly on the plot. Based on the presented example and other obtained results, it was noted that there is no correlation between the maximum strength and the maximum shear fatigue life within particular groups of bond types and at various bitumen amounts. Figure 11 shows, however, a visible influence of the type of the underlying surface (lower layer): AC or SMA.

Figure 12 shows a full comparison of results obtained at the preliminary laboratory stage for the tested combinations of interlayer bonds. The manner of presentation is analogous to Figure 11.

According to Figure 12 the strength and fatigue life of interlayer bonds depend on a combination of factors: the type of bitumen used in the tack coat and its amount and texture of the underlying layer. A tendency may be noted that softer bitumen improves the strength and shear fatigue life of the interface. The use of SBR polymer modification was neutral to bond performance. The texture of the underlying layer had the most pronounced impact on bonding quality. Specimens, in which, SMA 11 was used in the bottom layer, exhibited better properties than specimens in which AC 16 was used. Notably more advantageous results were obtained for specimens in which the lower layer had been milled, resulting in a grooved texture. This may be explained by a greater contact area, improved friction at the interface and better interlock between grains of the mixtures. Based on the above observations, the solutions with the modified bituminous emulsion C60BP3 70/100 + SBR tack coat were

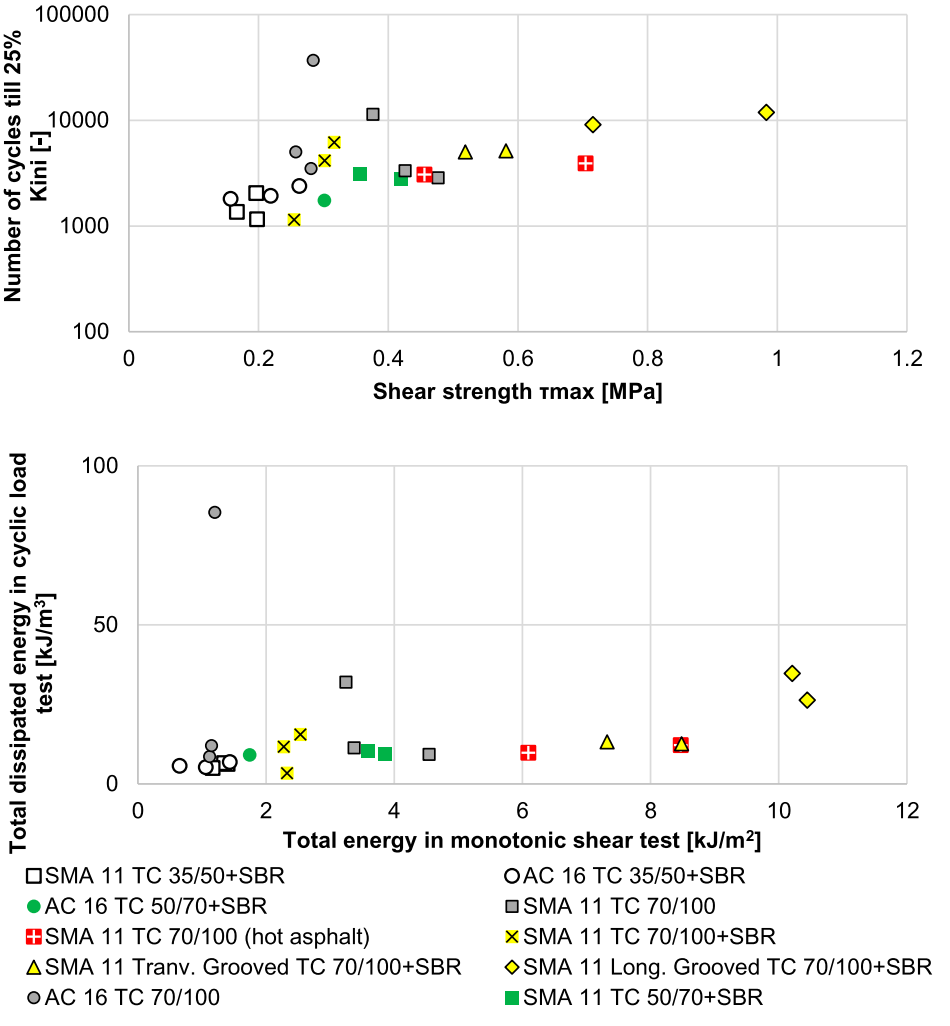

Figure 12. Results of monotonic and cyclic shearing tests of interfaces between poroelastic layers and the lower layers of AC 16 or SMA 11.

chosen for further full-scale tests. Also, because the influence of the amount of tack coat used during the laboratory tests on the obtained interlayer bonding results was not as strong as that of other factors (e.g. type of the lower layer, type of texture, type of bitumen emulsion), it was decided that a typical value of 0.2 kg/m^2 of bitumen residue will be used during the field trials, with a slightly increased value of 0.3 kg/m^2 in areas where milling of the newly laid binder layer was to be conducted. Various types of lower layers were investigated on the test sections: AC 16, SMA11, SMA 11 milled longitudinally as well as SMA 11 milled and covered with a reinforcement grid (Figure 3). To the best of the authors knowledge, the use of coarse grooved texture of the lower layer in combination with the poroelastic upper layer constitutes a novel solution, since in the decisive majority of PERS tests performed to date, the lower layer was either left with its natural texture or even especially smoothed using various methods.

Construction of test sections

The possibility of using ordinary asphalt batch plant, paver and compacting equipment for production, laying and compaction of SEPOR poroelastic wearing course was confirmed by previous positive

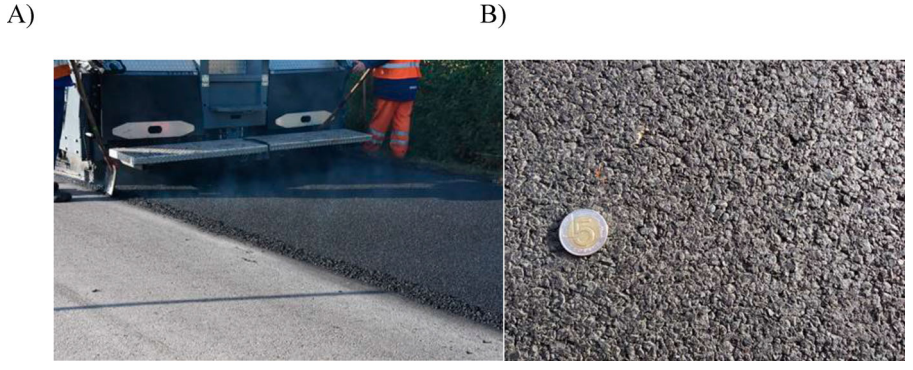

Figure 13. (A) Laying of the poroelastic mixture; (B) close-up view of the poroelastic wearing course.

Figure 14. Longitudinal marks caused by paver screed joints on the test sections.

observations in experimental field applications (Jaskula et al., 2020). The test Section 1 of poroelastic wearing course was next constructed on a private internal road loaded by tourist traffic where the purpose was to evaluate the effectiveness of different bonding techniques at the interface of poroelastic wearing course and the lower layer, to conduct initial experiments concerning noise reduction and to conduct fire tests concerning fuel spillages (Ejsmont et al., 2019; Jaskula et al., 2020). The test Section 2 with poroelastic wearing course SEPOR was constructed afterwards.

The main goals of the second test section were (1) to evaluate the performance of the designed poroelastic mixture in real traffic conditions, (2) to evaluate the possible influence of different lower layer types on the performance of the poroelastic mixture and (3) to conduct noise reduction tests at typical traffic speeds. Therefore, the second test section was located on a public road in Gdańsk – Galaktyczna street, which is subjected to constant and significant traffic – AADT = 1740 vehicles per lane, including 5% of heavy goods vehicles and buses. That corresponds to 0.5 million 100 kN axles per lane in 20 years. It was decided that the poroelastic mixture would be placed on a single lane of the two-way carriageway, so it was subjected to traffic in one direction. The width of the lane was 3 m. Because of the lack of intersections and exits, no turning movements occurred. The total length of this test section was 160 m. It was divided into eight subsections with a length of 20 m each that differed in terms of binder content in the poroelastic mixture, type of layer underneath and type of the bonding technique. Figure 13 shows the laying of the poroelastic mixture and close-up view of the ready made poroelastic weraing course.

The poroelastic wearing course for all subsections was placed and compacted during a single continuous pass of the paver to obtain uniform thickness and evenness. There was only one transverse construction joint, where laying and compaction of the second variant of the poroelastic mixture (with binder content of 13% instead of 11%) started. All the constructed variants are summarised in Figure 16.

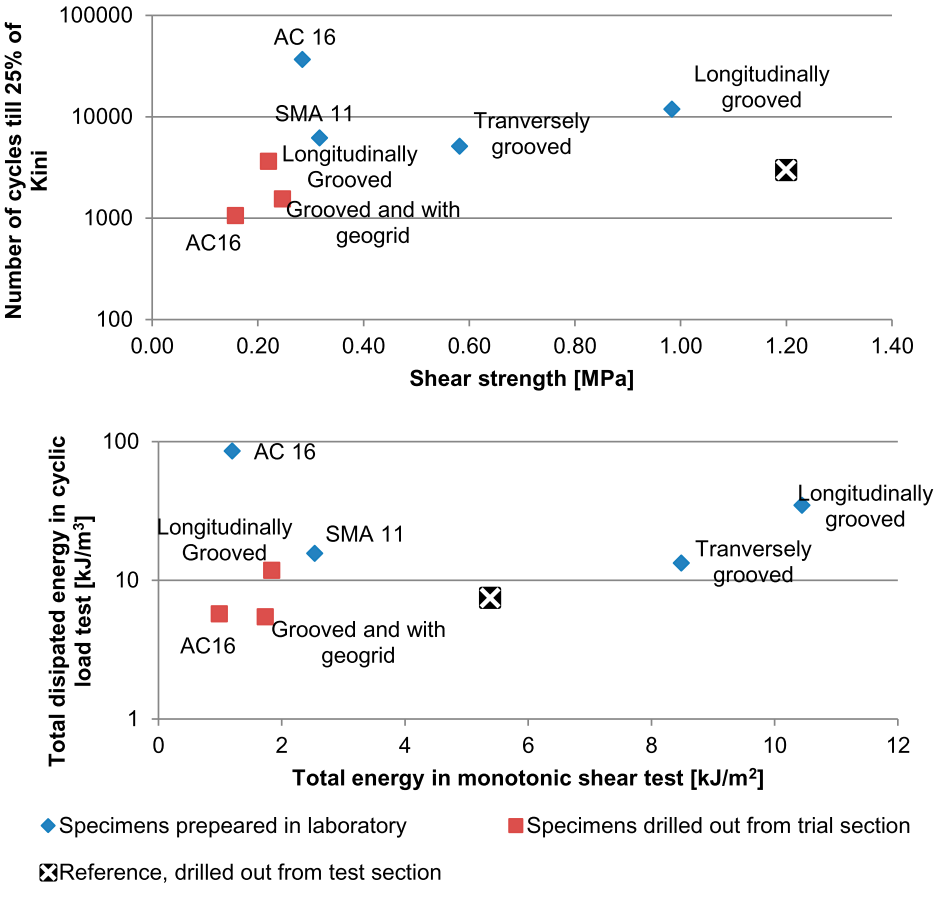

Figure 15. Comparison of results of monotonic shear test and cyclic shear load test obtained from specimens prepared in laboratory and specimens cored out from the test Section 1.

During construction of the test section, some irregularities on the surface of poroelastic layer occurred. Those irregularities were probably caused by inappropriate levelling of paver screed and are visible in Figure 14. It should be treated as a runtime construction technological error. Nevertheless, a typical HMA has a much greater tolerance due to the levelling of paver screed. Longitudinal marks were avoided in the part of the Section 2 by simply laying the poroelastic mixture with paving screed completely folded down. Such marks on the Section 1 could not be erased with a roller. Moreover, it was also completely impossible to pave manually or make manual corrections to the freshly laid mat (before compaction) without leaving significant marks. Accidental pickup of mixture that stuck to roller drum also resulted in permanent marks visible after rolling (see Figure 14).

Field evaluation of test sections

After construction of the test Section 1, specimens for evaluation of interlayer bonding quality were cored. Figure 15 shows a comparison of the results obtained for specimens cored from the test section with analogous layer interface combinations prepared earlier under laboratory conditions in the preliminary tests. In order to enable reference to bonds between typical asphalt mixtures, Figure 15 also shows the results obtained for bonding of AC 16 and SMA 8 (reference layers) laid at the same time on the test Section 1. The results in Figure 15 are presented in the same manner as in Figures 11 and 12.

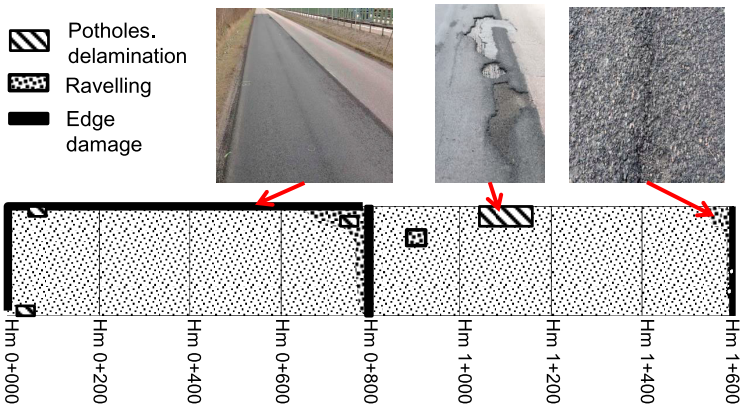

Subsection no.	1	2	3	4	5	6	7	8
Tack coat	Asphaltic emulsion C60 BP3 ZM 70/100 + SBR							
Amount of tack coat [kg/m^2]	0.2		0.3				0.2	
Type of upper layer	PSMA 5 CR 15 A11				PSMA 5 CR 15 A13			
Type of lower layer	AC 16	SMA 11	SMA 11 milled	SMA 11 milled + geogrid		SMA 11 milled	SMA 11	AC 16
Shear bond strength [MPa]	debonded	0.36	0.34	debonded	0.30	debonded	0.38	0.18

Figure 16. Plan of the test Section 2 with marked distresses and with results of bond shear strength of specimens cored out from the pavement.

It is visible in Figure 15 that the values of bonding parameters are lower for specimens cored from the test section than for specimens prepared in laboratory. This may result from considerable differences between compaction with road rollers and compaction in laboratory conditions (Jaskula, 2014), which, although not that apparent in the case of traditional asphalt mixes, become more pronounced in the case of poroelastic mixtures.

Shear strength of specimens cored in field is around two times lower than for specimens prepared in laboratory; difference in shear fatigue life is several folds. Shear strength of reference interlayer bond of traditional mixtures is also several times higher. However, it is noteworthy that shear fatigue life of specimens with poroelastic top layer subjected to cyclic shear loading is comparable to that of the reference AC 16 and SMA 8 interface. Likewise, as visible in Figure 15(b), the dissipated energy in cyclic shear test is similar for poroelastic layer bonds and the reference bond.

It is worthwhile to perform a more detailed comparison between the results for specimens containing poroelastic top layers and the reference specimens of typical SMA 8 and AC 16 interfaces. The reference interlayer bond exhibits shear strength around 1.2 MPa, which is significantly higher than shear strength values registered for specimens with poroelastic layer. Nevertheless, shear fatigue life expressed in the number of shear cycles to failure $N_{25\%}$ is similar for reference bonds and the bonds with poroelastic top layer laid over grooved surface of the lower layer. Energy needed for complete failure of the reference interlayer bond under monotonic shear test is lower than respective energy measured for bond between poroelastic layer and grooved lower layer. These observations suggest that parameters, such as total energy in monotonic direct shear test or bond shear fatigue life in cyclic shear test with normal stress, may reflect the actual performance of interlayer bond more accurately than its shear strength.

Field research has confirmed that milling of the surface and the resultant increase in the contact area at the interface between layers leads to improvement in shear strength and shear fatigue life of

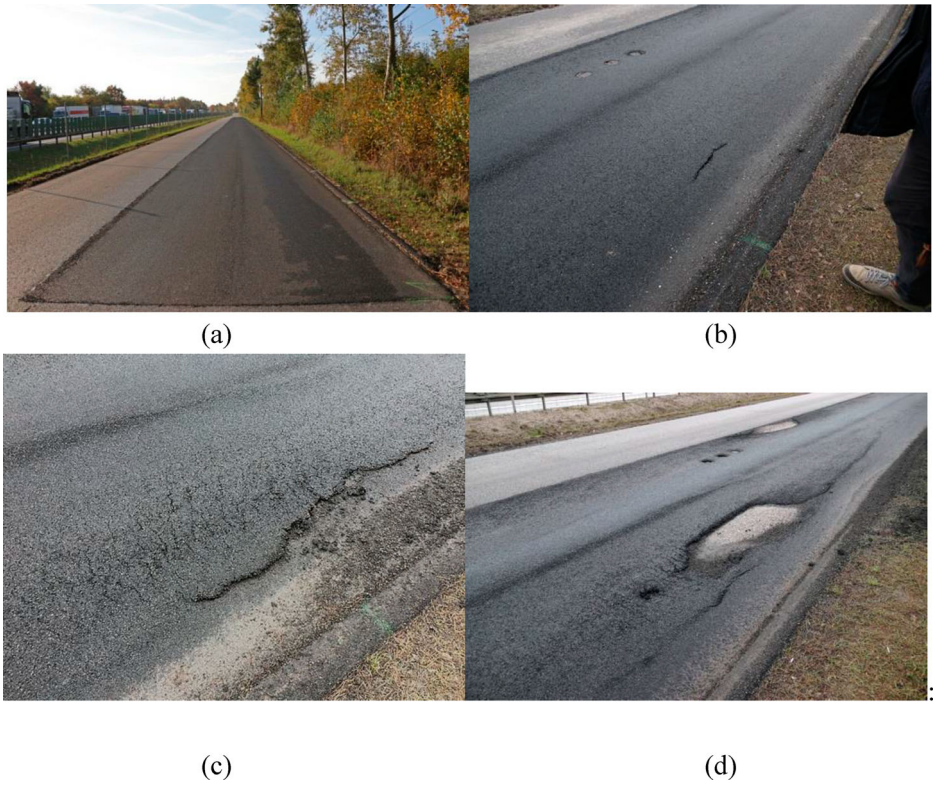

Figure 17. Deterioration of the first subsection of the test Section 2: (a) 15 October 2019 (13th day); (b) 5 February 2020 (126th day); (c) 19 February 2020 (140th day); (d) 10 March 2020 (160th day).

the bond. Throughout 360 days of its service, the test Section 1 did not exhibit any signs of distress resulting from loss of bonding between the poroelastic layer and the lower layer. The only observed distress was significant ravelling of the poroelastic layer, resulting in dislodgement of mineral aggregate and crumb rubber particles from the top zone (around 1 cm) of the poroelastic wearing course. Insufficient bitumen content in the mix was identified as the primary cause of the observed intensive ravelling. The problem was eliminated on the test Section 2 through an increase in bitumen content. It should be noted that due to its location on a vehicle manoeuvring area, the section 1 was subjected to shearing forces generated by wheel turns and horizontal forces from braking and accelerating – nevertheless, loss of interlayer bonding did not occur. Even during deconstruction of the test pavement, it proved impossible to separate the layers manually or mechanically. The poroelastic layer was finally only removed by milling.

The test Section 2 consisted of 8 subsections with varying interlayer bond combinations and two levels of bitumen contents in the poroelastic mixture. A scheme of the test section is presented in Figure 16. Lack of interlayer bonding was noted during coring on some subsections – the specimens delaminated. Average shear strength values of specimens that did not delaminate during coring are compared in Figure 15. The lowest average shear strength (based on two measurements) was observed on subsection 8 with AC 16 lower layer and equalled 0.18 MPa. The highest average shear strength values were obtained on two subsections with SMA 11 lower layers – 0.36 and 0.38 MPa. Interestingly, on the test section 2 milling before placement of the wearing course did not noticeably improve the shear strength.

Figure 16 shows also the extent of distress visible on the test section after 170 days of service. On the section 2 distress resulting from loss of interlayer bonding was observed. On all the subsections

Figure 18. Deterioration of the sixth subsection of the test Section 2: (a) 22 November 2019 (51st day); (b) 13 January 2020 (103rd day); (c) 5 February 2020 (126th day); (d) 19 February 2020 (140th day); (e) 4 March 2020 (154th day); (f) 10 March 2020 (160th day).

where distress associated with poroelastic layer slippage was visible, loss of bonding was noted during coring. The process of damage development was registered and it is presented in subsequent photos in Figures 17 and 18. Usually the mechanism was similar – appearance of the crack due to loss of internal cohesion of the mixture, stripping of the loose mixture material, loss of interlayer bonding with the lower layer, appearance of the pothole and, consequently, further loss of the mixture material. Interestingly, this phenomenon was very rapid. In the first section, it only took 1 month to develop a pothole with layer deformation from a single crack. It is an important fact that on other subsections, where interlayer shear strength (between the poroelastic wearing curse and the binder layer) was greater than 0.3 MPa, no distress was observed.

After 170 days of service the test Section 2 was deconstructed due to danger of damage to vehicles using the road. The Section 1 operated for 360 days, according to the research schedule.

Conclusions and recommendations

Based on the material presented in this paper, the following conclusions have been drawn:

(1) Bonding quality between the poroelastic SEPOR-PSMA5 wearing course and the HMA binder course is significantly lower than bonding between typical pavement layers. Shearing strength in monotonic direct shear loading test ranges from 0.18 to 1.0 MPa for specimens prepared in laboratory conditions and from 0.18 to 0.38 MPa for specimens cored from pavement. The strength is up to 3 times lower in comparison to reference bonding of AC 16 and SMA 8. It should be noted that in-layer shearing strength of the poroelastic layer lies within the range of 0.3–0.8 MPa.

(2) Analysis of test results indicates that shear strength is not a sufficiently accurate measure of durability and quality of bonding between the poroelastic layer with the underlying layer. Determination of the total energy needed for full shearing failure of the interface in monotonic direct shearing test or performance of cyclic load shearing test in the AST device is recommended.
(3) Twenty-seven combinations of layer interfaces were tested in laboratory and the best effects were obtained for poroelastic SEPOR-PSMA5 wearing course laid over SMA 11 after longitudinal milling and spraying of the grooved surface with modified bituminous emulsion based on soft bitumen 70/100 at 0.3 kg/m^2.
(4) Eight selected combinations of layer interfaces were constructed in field sections. The best effects were obtained for poroelastic SEPOR-PSMA5 wearing course over SMA 11 with modified bituminous emulsion tack coat based on soft bitumen 70/100. However, there was no pronounced improvement of interlayer bonding due to milling of the lower layer.
(5) Premature distress of pavements with poroelastic wearing course on two test sections was not generally caused by problems with interlayer bonding, apart from local losses of bonding noted on one test section. During deconstruction works on both test sections, it proved impossible to separate the poroelastic layer by manual or mechanical means, save by the use of a road milling machine. The primary cause of premature distress on both test sections was ravelling in whole part of Section 1 and in local parts of Section 2.

After the initial laboratory test of interlayer shear bond quality and after observations performed on the two test sections, the following recommendations have been formulated:

- The lower layer, located directly below the poroelastic wearing course, should be constructed from SMA. Milling of lower layers is also recommended.
- Tack coat should contain softer bitumen. In this study, polymer-modified bituminous emulsion with bitumen 70/100 provided better quality of the interlayer bond than remaining tack coats.
- The technology is very sensitive to the construction process and control. Properly produced tack coat and milled texture of the lower layer are not enough to ensure appropriate interlayer bonding. Insufficient compaction or overly flexible lower layer can lead to the loss of friction between poroelastic wearing course and lower layer. Any manual corrections during laying of the poroelastic layer must be avoided.

Acknowledgements

Research work reported in this article was sponsored by the Polish National Centre for Research and Development (NCBiR) under project SEPOR (Grant TECHMATSTRATEG1/347040/17/NCBR/2018).

Disclosure statement

No potential conflict of interest was reported by the author(s).

Funding

This work was supported by Narodowe Centrum Badań i Rozwoju BadaÅ, i Rozwoju [grant number TECHMATSTRATEG 1/347040/17/NCBR/2018].

ORCID

P. Jaskula http://orcid.org/0000-0002-1563-2778
D. Rys http://orcid.org/0000-0002-7252-8002
C. Szydłowski https://orcid.org/0000-0002-6141-9839
M. Stienss https://orcid.org/0000-0003-1811-1086
L. Mejlun https://orcid.org/0000-0001-6456-7645
M. Jaczewski https://orcid.org/0000-0003-4722-2957
G. Ronowski https://orcid.org/0000-0002-2448-480X

References

Bendtsen, H. (2015). Performance of PERS. *Final PERSUADE Seminar*.

Crispino, M., Festa, B., Giannattasio, P., & Nicolosi, V. (1997). *Evaluation of the interaction between the asphalt concrete layers by a new dynamic test*. Eighth International Conference on Asphalt Pavements, Seattle USA, 10-14 August.

D'Andrea, A., Tozzo, C., Boschetto, A., & Bottini, L. (2013). Interface roughness parameters and shear strength. *Modern Applied Science*, *7*(10), 1–10.

Donovan, E. P., Al-Qadi, I. L., & Loulizi, A. (2000). Optimization of tack coat application rate for geocomposite membrane on bridge decks. *Transportation Research Record: Journal of the Transportation Research Board*, *1740*(1), 143–150. https://doi.org/10.3141/1740-18

Ejsmont, J. A., Goubert, L., Ronowski, G., & Swieczko-Zurek, B. (2016). Ultra low noise poroelastic road surfaces. *Coatings*, *6*(2), 18–15. https://doi.org/10.3390/coatings6020018

Ejsmont, J., Mioduszewski, P., Ronowski, G., Taryma, S., & Świeczko-Żurek, B. (2015). *Final report on noise and rolling resistance* (pp. 1–37). Gdansk: Gdanksk University of Technology Research project report

Ejsmont, J., Sandberg, U., Swieczko-Zurek, B., & Mioduszewski, P. (2014a). Tyre / road noise reduction by a poroelastic road surface. Inter noise 2014, 43rd International Congress on Noise Control Engineering, Meulborne, Australia, November 16-19.

Ejsmont, J., Świeczko-Żurek, B., Ronowski, G., & Taryma, S. (2014b). *Intermediate report on rolling Resistance*. Gdansk: Gdansk University of Technology Research project report.

Ejsmont, J., Swieczko-Zurek, B., & Jaskula, P. (2019). *Low noise poroelastic road pavements based on bituminous*. Nois-Con 2019, National Conference on Noise Control Engineering, San Diego, USA, 26-28 August.

Ejsmont, J., Świeczko-Żurek, B., Owczarzak, W., Sommer, S., & Ronowski, G. (2018). Tire / road noise on poroelastic road surfaces. 11th European Congress and Exposition on Noise Control Engineering, Crete, 27-31 May.

FGSV. (1999). *Merkblatt für schichtenverbund, nähte, anschlüsse, randausbildung von verkehrsflächen aus asphalt*. Forschungsgesellschaft für S traßen- und Verkehrswesen (FGSV).

Górszczyk, J., & Malicki, K. (2012). Influence of the tack coat material on interlayer bonding properties in asphalt layers system. In TI-Swedish National Road and Transport Research Institute (Ed.), *Proceedings of the 4th European Pavement and Asset Management Conference EPAM 2012*. TI-Swedish National Road and Transport Research Institute.

Goubert, L., & Sandberg, U. (2009). Development of the ultra low noise poroelas- Tic road surface: the findings of the persuade project. In *23rd International Congress on Sound & Vibration* (pp. 1–8). International Institute of Acoustics and Vibration (IIAV)

Hakimzadeh, S., Kebede, N. A., Buttlar, W. G., Ahmed, S., & Exline, M. (2012). Development of fracture-energy based interface bond test for asphalt concrete. *Road Materials and Pavement Design*, *13*(S1), 76–87. https://doi.org/10.1080/14680629.2012.657059

Jaskula, P. (2014). *Influence of compaction effectiveness on interlayer bonding of asphalt layers*. The 9th International Conference "ENVIRONMENTAL ENGINEERING." (p. 7) Vilnius: VGTU Press.

Jaskula, P. (2018). *Sczepność warstw asfaltowych w wielowarstwowych układach nawierzchni drogowych (wydawnictw)*. Gdansk: Gdansk University of Technology.

Jaskula, P., Ejsmont, J., Stienss, M., Ronowski, G., Szydlowski, C., Swieczko-Zurek, B., & Rys, D. (2020). Initial field validation of poroelastic pavement made with crumb rubber, mineral aggregate and highly polymer-modified bitumen. *Materials*, *13*(6), https://doi.org/10.3390/ma13061339

Jaskula, P., Szydlowski, C., Stienss, M., Rys, D., & Jaczewski, M. (2019). Durable poroelastic wearing course SEPOR with highly modified bitumen. In *AIIT International Congress on Transport Infrastructure and Systems in a Changing World, TIS Roma 2019* (pp. 882–889). Roma: Elsevier.

Jaskula, P., Szydlowski, C., Stienss, M., Rys, D., Jaczewski, M., & Pszczola, M. (2020). Durable poroelastic wearing course SEPOR with highly modified bitumen. In *Transportation Research Procedia* (Vol. 45 pp. 882–889). Elsevier B.V.

Jia, X., & Huang, B. (2015). *An energy-based approach to evaluate the shear resistance of pavement interlayer utilizing shear test*. 6th Conference of the European Asphalt Technology Association (p. 15-17 June23). Stokholm.

Kalman, B., Biligiri, K. P., & Sandberg, U. (2011). Project PERSUADE: Optimization of poroelastic road surfaces in the laboratory. In *Inter noise 2011* (pp. 1–9). Institute of Noise Control Engineering/Japan & Acoustical Society of Japan.

Kruntcheva, M. R., Collop, A. C., & Thom, N. H. (2004). Feasibility of Assessing Bond Condition of Asphalt Concrete layers with Dynamic Nondestructive testing. *Journal of Transportation Engineering*, *130*(4), 510–518. https://doi.org/10.1061/(ASCE)0733-947X(2004)130:4(510)

Lu, G., Renken, L., Li, T., Wang, D., Li, H., & Oeser, M. (2019). Experimental study on the polyurethane-bound pervious mixtures in the application of permeable pavements. *Construction and Building Materials*, *202*, 838–850. https://doi.org/10.1016/j.conbuildmat.2019.01.051

Meiarashi, S. (2004). Porous elastic road surface as urban highway noise measure. *Transportation Research Record*, *1880*(1), 151–157. https://doi.org/10.3141/1880-18

Mohammad, L., Bae, A., Elseifi, M., Button, J., Scherocman, J. A., Mohammad, L., & Patel, N. (2009). Interface shear strength characteristics of emulsified tack coats. *AAPT Annual Meeting*, *78*, 249–279.

Raab, C., & Partl, M. N. (1998). Shear strength properties between asphalt pavement layers. *Archives of Civil Engineering*, *vol. 44*(Issue 3), 353–365.

Ragni, D., Canestrari, F., Allou, F., Petit, C., & Millien, A. (2020). Shear-torque fatigue performance of Geogrid-reinforced asphalt interlayers. *Sustainability (Switzerland)*, *12*(11), 4381–4321. https://doi.org/10.3390/su12114381.

Recasens, M. R., Martinez, A., & Jimenez, F. P. (2006). Evaluation of the effect of heat-adhesive emulsions for tack coats with shear test from the road Research laboratory of barcelona. *Transportation Research Record: Journal of the Transportation Research Board*, *1970*(1), 64–70. https://doi.org/10.1177/0361198106197000106

Romanoschi, S. A., & Metcalf, J. B. (2001). Effects of interface condition and horizontal wheel loads on the life of flexible pavement structures. *Transportation Research Record: Journal of the Transportation Research Board*, *1778*(1), 123–131. https://doi.org/10.3141/1778-15

Sandberg, U. (2015). PERS – A historical review. *Final PERSUADE Seminar*.

Sandberg, U., Goubert, L., Biligiri, K. P., & Kalman, B. (2010). *State-of-the-Art regarding poroelastic road surface, WP 8 information management*.

Sholar, G. A. (2004). *Testing of bond strength between asphalt layers*. In AAPT.

Srirangam, S. K., Anupam, K., Casey, D., Liu, X., Kasbergen, C., Scarpas, A., & Kingdom, U. (2016). Evaluation of structural performance of poro-elastic road surfacing pavement subjected to rolling truck Tire loads. *Transportation Research Record: Journal of the Transportation Research Board, (November 2015)*, 2591(1), 1–25. https://doi.org/10.3141/2591-07

Świeczko-Żurek, B., Ejsmont, J., Motrycz, G., & Stryjek, P. (2015). Risks related to car fire on innovative poroelastic road surfaces—PERS. *FIRE AND MATERIALS*, *39*(2), 95–108. https://doi.org/10.1002/fam.2231

Świeczko-Żurek, B., Goubert, L., Ejsmont, J. A., & Ronowski, G. (2018). *Poroelastic road surfaces state of The Art*. *Proceedings of the Rubberized Asphalt Asphalt Rubber 2018 Conference*. (pp. 625–643).

Wang, D., Liu, P., Leng, Z., Leng, C., Lu, G., Buch, M., & Oeser, M. (2017). Suitability of PoroElastic Road Surface (PERS) for urban roads in cold regions: Mechanical and functional performance assessment. *Journal of Cleaner Production*, *165*(July), 1340–1350. https://doi.org/10.1016/j.jclepro.2017.07.228

Zofka, A., Bernier, A., Josen, R., & Maliszewski, M. (2014 August). Advanced shear tester for solid and layered samples. *Asphalt Pavements*, 405–420. https://doi.org/10.1201/b17219

Zofka, A., Maliszewski, M., Bernier, A., Josen, R., Vaitkus, A., & Kleizienė, R. (2015). Advanced shear tester for evaluation of asphalt concrete under constant normal stiffness conditions. *Road Materials and Pavement Design*, *16*(sup1), 187–210. https://doi.org/10.1080/14680629.2015.1029690